INL/JOU-16-40072-Revision-0

Re-evaluation of Neptunium-Nitric Acid Radiation Chemistry by Multi-Scale Modelling

Travis S. Grimes, Bruce J. Mincher,
Stephen P. Mezyk, Gregory P. Horne

November 2016

The INL is a U.S. Department of Energy National Laboratory
operated by Battelle Energy Alliance

INL/JOU-16-40072-Revision-0

Re-evaluation of Neptunium-Nitric Acid Radiation Chemistry by Multi-Scale Modelling

Travis S. Grimes, Bruce J. Mincher, Stephen P. Mezyk, Gregory P. Horne

November 2016

Idaho National Laboratory
Idaho Falls, Idaho 83415

http://www.inl.gov

Prepared for the
U.S. Department of Energy

Under DOE Idaho Operations Office
Contract DE-AC07-05ID14517

Re-evaluation of Neptunium-Nitric Acid Radiation Chemistry by Multi-Scale Modelling

G. P. Horne[1,2,*], T. S. Grimes[3], B. J. Mincher[3], and S. P. Mezyk[1]

[1]*California State University at Long Beach, Long Beach, CA 90804, USA.*

[2]*Radiation Research Laboratory, University of Notre Dame, Notre Dame, IN 46556, USA.*

[3]*Idaho National Laboratory, Idaho Falls, ID, P.O. Box 1625, 83415, USA.*

* Corresponding author.

ABSTRACT

Multi-scale modelling has been used to quantitatively reevaluate the radiation chemistry of neptunium in a range of aerated nitric acid solutions (0.1 – 6.0 mol dm^{-3}). Exact calculation of initial radiolytic yields accounting for changes in radiation track chemistry was found to be crucial for reproducing experimental data. The gamma irradiation induces changes in the Np(VI):Np(V) oxidation state distribution, predominantly driven by reactions involving HNO_2, H_2O_2, $NO_2^{\bullet}$, and $NO_3^{\bullet}$ from the radiolysis of aqueous nitric acid. Oxidation of Np(V) by $NO_3^{\bullet}$ ($k = 8.1 \times 10^8$ dm^3 mol^{-1} s^{-1}) provides the initial increase in Np(VI) concentration, whilst also delaying net reduction of Np(VI) by consuming HNO_2. Reduction of Np(VI) is dominated by thermal reactions with HNO_2 ($k = 0.7 - 73$ dm^3 mol^{-1} s^{-1}) and H_2O_2 ($k = 1.9$ dm^3 mol^{-1} s^{-1}). A steady-state is eventually established once the concentration of Np(V) is sufficiently high enough to be oxidized by $NO_2^{\bullet}$ ($k = 2.4 \times 10^2 - 3.1 \times 10^4$ dm^3 mol^{-1} s^{-1}). An additional thermal oxidation reaction between Np(V) and HNO_3 ($k = 2.0 \times 10^3$ dm^3 mol^{-1} s^{-1}) is required for nitric acid concentrations >4.0 mol dm^{-3}. For 0.1 mol dm^{-3} HNO_3, the rate of Np(VI) reduction is in excess of that which can be accounted for by radiolytic product mass balance, suggesting the existence of a catalytic acid dependent reduction process.

INTRODUCTION

Current used nuclear fuel (UNF) reprocessing methods use hydro-based techniques in the form of solvent extraction. This approach involves initial dissolution of UNF in concentrated nitric acid (HNO_3) to yield a highly radioactive acidic liquor, from which desired metal ions (e.g. uranium, plutonium, and neptunium) are partitioned into an organic phase, comprising of specialized extractants (e.g. tributyl phosphate (TBP) or N,N,N',N'- tetraoctyl diglycolamide (TODGA) dissolved in an organic diluent (e.g. odorless kerosene or *n*-dodecane), and subsequently into appropriate product and waste streams. Successful partitioning and separation relies on the formation and maintenance of particular metal ion valence states amenable to complexation by the extractants used in a given process. For example, in the *Plutonium Uranium*

Reduction EXtraction (PUREX) process, neptunium is well extracted by TBP when it is tetravalent (Np(IV)) and hexavalent (Np(VI)), but almost unextractable when pentavalent (Np(V)). However, under anticipated large-scale process conditions the solvent system would be continuously subjected to an intense multi-component radiation field, which would induce radiolytic degradation of the solvent components. Such degradation results in the formation of a variety of oxidizing and reducing radicals and other species, many of which are particularly problematic for redox-active metals such as neptunium as they can alter oxidation state distributions, ultimately affecting the separation efficiency of reprocessing systems.

Irradiation of a given neptunium-nitric acid solution typically results in the formation of a mixed valency system, regardless of the solutions initial neptunium valencies.[1] Under process conditions, Np(V) and Np(VI) are the predominant oxidation states, with their distribution often described by equation (**1**).[2]

$$2\mathrm{Np(V)} + \mathrm{NO_3^-} + 3\mathrm{H_{aq}^+} \rightleftharpoons 2\mathrm{Np(VI)} + \mathrm{HNO_2} + \mathrm{H_2O} \qquad (\mathbf{1})$$

This empirical description provides little insight into the radiolytic species truly involved in establishing the neptunium valency distribution, whilst also giving no indication of radiation dependency, e.g. radiation quality (energy and type of radiation) and absorbed dose.

Recent investigations by Mincher *et al.*[1] found that gamma irradiation of predominantly Np(VI) in a 4.0 mol dm^{-3} HNO_3 solution underwent oxidation, followed by reduction, to yield a mixed valency system of Np(V) and Np(VI). A combination of experimental measurements and kinetic modelling allowed for identification of the most important chemical reactions (**2** – **5**) responsible for influencing the oxidation state distribution in this particular system:

(i) At low applied gamma dose, an initial increase in Np(VI) concentration was observed due to oxidation of small amounts of Np(V) by the action of the oxidizing products of nitric acid radiolysis; i.e. the nitrate radical ($NO_3^{\bullet}$) and/or the hydroxyl radical ($OH^{\bullet}$).

$$\mathrm{Np(V)} + \mathrm{OH^{\bullet}} \rightarrow \mathrm{Np(VI)} + \mathrm{OH^-} \qquad (\mathbf{2})$$

$$\mathrm{Np(V)} + \mathrm{NO_3^{\bullet}} \rightarrow \mathrm{Np(VI)} + \mathrm{NO_3^-} \qquad (\mathbf{3})$$

(ii) The net reduction of Np(VI) was found to only occur after a sufficiently high concentration of nitrous acid (HNO_2) had accumulated in the system. Calculations

also showed that reduction by hydrogen peroxide (H_2O_2) is an important pathway, and that both Np(VI) reduction processes exhibit slow kinetics.

$$Np(VI) + HNO_2 \rightarrow Np(V) + NO_2^{\bullet} + H_{aq}^{+} \quad (4)$$

$$Np(VI) + H_2O_2 \rightarrow Np(V) + HO_2^{\bullet} + H_{aq}^{+} \quad (5)$$

These findings were in broad agreement with previous calculations of irradiated Np(V)/Np(VI) reported by Vladimirova.[3] However, despite both kinetic modelling investigations arriving at similar conclusions through using comparable neptunium reaction sets, very different rate coefficients for the key reactions driving the valency distribution in 4.0 mol dm^{-3} nitric acid solutions, outlined in Table 1, were deduced. Furthermore, multiple other rate coefficients reported by Vladimirova[3] for other nitric acid concentrations changed quite drastically, which indicates that the kinetic modelling data set may not have been complete.

Table 1. Optimized literature rate coefficients from kinetic modelling studies for key neptunium reactions in 4.0 mol dm^{-3} nitric acid solutions.

Reference	**rate coefficient** (dm^3 mol^{-1} s^{-1})		
	$Np(VI) + HNO_2$	$Np(VI) + H_2O_2$	$Np(V) + NO_3^{\bullet}$
Mincher *et al.* [1]	0.7	20	8.1×10^8
Vladimiorva [3]	0.8	4	1.0×10^5

Our current understanding of neptunium redox chemistry in the presence of a radiation field has been constrained to qualitative or empirical mechanistic explanations, as a consequence of previous modelling attempts that employed conservative reaction sets, estimated initial radiolytic yields, and used empirical fitting functions to obtain agreement with experimental data. These approaches provide limited quantitative mechanistic information and thus do not provide the necessary confidence for decisions in the development and implementation of advanced reprocessing schemes. In response to this, the presented research quantitatively re-evaluates the radiation chemistry of neptunium in aerated aqueous solutions of nitric acid under a range of conditions relevant to largescale process conditions, by utilizing a multi-scale modelling approach.

The importance of using representative initial radiolytic yields to model the radiation chemistry of complex aqueous solutions has recently been demonstrated by Horne *et al.*[4], who used multi-scale modelling to show that initial yields were crucial for determining the speciation and magnitude of radiolytic species (both oxidizing and reducing) entering bulk solution, which in turn determines the outcome of steady-state radiation chemistry. In this study the multi-scale modelling approach utilizes a far more comprehensive chemical reaction set than those previously published, and re-evaluates the rate coefficients reported by Mincher *et al.*[1] and Vladimirova[3], to determine their accuracy and applicability to a range of neptunium and nitric acid concentrations. Our study demonstrated that the important reactions and their associated rate coefficients are strongly dependent upon the initial radiolytic yields, and that previous efforts were incomplete due to them not taking into account variations in radiation track chemistry. We report new experimental data, accompanied by multi-scale modelling interpretations, on the radiochemical behavior of neptunium for nitric acid concentrations over the range of 0.1 to 6.0 mol dm^{-3}.

METHODS

Multi-scale Modelling

The multi-scale modelling approach uses a combination of stochastic and deterministic methodologies to model complex irradiated systems.[4] This approach breaks down the overall calculation into four stages corresponding to different time (and distance) regimes: radiation track structure formation (<1 fs), physicochemical processes (<1 ps), nonhomogeneous reaction kinetics (<1 μs), and homogeneous bulk chemistry (>1 μs).

The stochastic component was used to calculate a set of initial, indirect effect, radiolytic yields for the products of water radiolysis from the point of energy deposition to complete spatial relaxation of the radiation chemical track.[5-7] The radiolytic yields at 10 μs, in conjunction with those for direct effects[8], were corrected for the respective electron fractions of water, nitrate, and nitric acid and subsequently evaluated by the deterministic component of the multi-scale model, allowing calculation of the formation rates of the products of radiolysis.

The deterministic model for bulk homogeneous radiation chemistry draws upon an extensive water, nitrate, and nitric acid chemical reaction set expressed as coupled kinetic differential

equations[4] which were solved by the FACSIMILE software package. For the purposes of this work the reaction set was supported by incorporating supplementary neptunium reactions given in Table 2.

Table 2. Supporting neptunium reactions and rate coefficients used in the multi-scale modelling approach.

chemical reaction	**rate coefficient** ($dm^3\ mol^{-1}\ s^{-1}$)	**Reference**
$2Np(V) + 4H_{aq}^{+} \rightleftharpoons Np(IV) + Np(VI) + 2H_2O$	$k_f = 2.67 \times 10^{-5}$ $k_b = 4.5 \times 10^{-2}$	9
$Np(V) + HNO_3 \rightarrow Np(VI) + HNO_3^-$	**2.0×10^{-3}**	**this work**
$Np(V) + OH^{\bullet} \rightarrow Np(VI) + OH^-$	4.7×10^{8}	10
$Np(V) + e_{aq}^- \rightarrow Np(IV)$	5.0×10^{9}	11
$Np(V) + H^{\bullet} \rightarrow Np(IV) + H_{aq}^{+}$	5.0×10^{6}	11
$Np(V) + NO_3^{\bullet} \rightarrow Np(VI) + NO_3^-$	**8.1×10^{8}**	**1 and this work**
$Np(V) + NO_2^{\bullet} \rightarrow Np(VI) + NO_2^-$	**$2.4 \times 10^{2} – 3.1 \times 10^{4}$**	**12 and this work**
$Np(V) + O^{\bullet -} + H_2O \rightarrow Np(VI) + OH^{\bullet} + OH^-$	4.7×10^{8}	11
$Np(V) + H_2O_2 \rightarrow Np(VI) + OH^{\bullet} + OH^-$	0.45	11
$Np(V) + H_2O_2 \rightarrow Np(IV) + OH^{\bullet} + OH^-$	5.65×10^{-2}	11
$Np(V) + HO_2^{\bullet} \rightarrow Np(IV) + O_2 + H_{aq}^{+}$	1.1×10^{3}	11
$Np(IV) + OH^{\bullet} \rightarrow Np(V) + OH^-$	3.2×10^{8}	11
$Np(IV) + H^{\bullet} \rightarrow Np(III) + H_{aq}^{+}$	1.0×10^{6}	11
$Np(IV) + NO_3^{\bullet} \rightarrow Np(V) + NO_3^-$	2.0×10^{5}	12
$Np(IV) + H_2O_2 \rightarrow Np(V) + OH^{\bullet} + OH^-$	8×10^{-2}	11
$Np(VI) + e_{aq}^- \rightarrow Np(V)$	2.3×10^{10}	11
$Np(VI) + H^{\bullet} \rightarrow Np(V)$	4.0×10^{8}	1
$Np(VI) + H_2O_2 \rightarrow Np(V) + HO_2^{\bullet} + H_{aq}^{+}$	**1.9**	**this work**
$Np(VI) + HNO_2 \rightarrow Np(V) + NO_2^{\bullet} + H_{aq}^{+}$	**0.7 – 73**	**this work**
$Np(VI) + HO_2^{\bullet} \rightarrow Np(V) + O_2 + H_{aq}^{+}$	6.8×10^{4}	11
$Np(VI) + O_2^{\bullet -} \rightarrow Np(V) + O_2$	6.8×10^{4}	11

Experiments

Neptunium Sample Preparation. Neptunium solutions were prepared from on-hand acidic nitrate stock solutions at the Idaho National Laboratory. Predominantly Np(VI) stock solutions were prepared by dissolution of neptunium-237 hydroxide in concentrated nitric acid, followed by subsequent volume reduction cycles and redissolution in dilute nitric acid.

Gamma Irradiations. Gamma irradiations were performed using a Nordion Gammacell 220E ^{60}Co Source Unit at the Idaho National Laboratory. Samples consisting of <1 mL of air saturated neptunium-nitric acid solution sealed in quartz cuvettes, were subjected to doses up to 40 kGy. Dosimetry was determined using Fricke solution[13] and subsequently corrected for ^{60}Co decay ($\tau_{1/2}$ = 5.27 years).

Analytical Procedure. UV-Vis spectroscopy *(Cary 6000 UV/Vis absorption spectrophotometer*) was used to simultaneously determine the concentrations of Np(V) (λ_{max} = 981 nm) and Np(VI) (λ_{max} = 1225 nm) immediately following the sealed cuvette irradiation.

RESULTS AND DISCUSSION

Re-evaluation of the Gamma Irradiation of Neptunium in 4.0 mol dm^{-3} Nitric Acid. The neptunium data reported by Mincher *et al.*[1] for the gamma radiolysis of 4.0 mol dm^{-3} HNO_3 is given in **Figure 1**. Plotted alongside the literature data are predictions from the multi-scale calculations performed in this work. The very good agreement with the experimental data could only be attained through the use of stochastically calculated initial radiolytic yields representative of the system in question, as opposed to the static values used by Mincher *et al*. A comparison of these initial yields is given in **Table 3**.

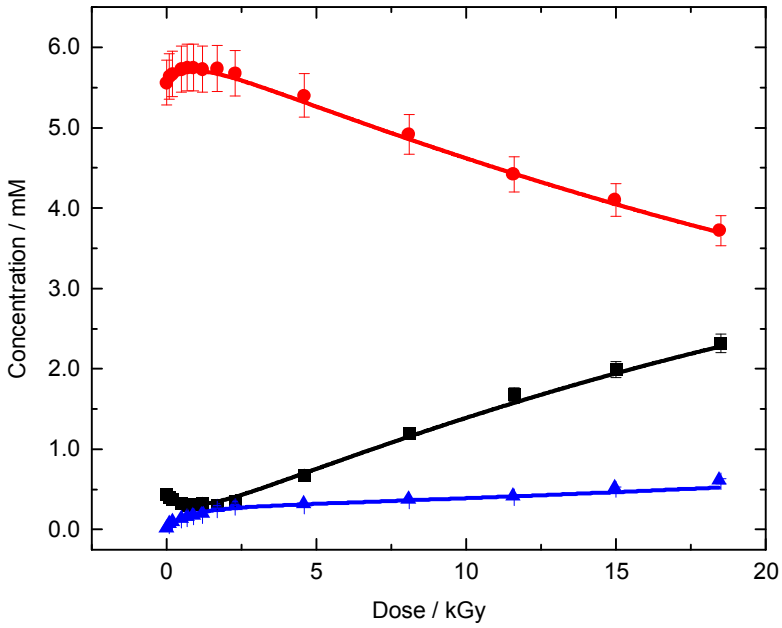

Figure 1. Concentration of Np(V)(■), Np(VI)(●), and HNO_2 (▲) (±5% error bars) as a function of absorbed dose from the gamma radiolysis (2.13 Gy s^{-1}) of 4.0 mol dm^{-3} HNO_3 + 6×10^{-3} mol dm^{-3} Np (reference 1**)**. Solid lines are predicted values from multi-scale modelling calculations.

Analysis of these initial G-values highlights a number of mechanistic inaccuracies in the previous modelling attempts. Firstly, at high HNO_3 concentrations (>1 mol dm^{-3}) no $OH^{\bullet}$ survives the initial radiation track chemistry due to it being predominantly scavenged by undissociated HNO_3 ($pK_a \sim 1.37$), which has an initial concentration of 0.54 mol dm^{-3} in 4 mol dm^{-3} HNO_3.[14]

$$HNO_3 + OH^{\bullet} \rightleftharpoons NO_3^{\bullet} + H_2O \qquad k_f = 1.9 \times 10^7 \text{ dm}^3 \text{ mol}^{-1} \text{ s}^{-1} \qquad \textbf{(16)}^{15}$$

$$k_b = 3.0 \times 10^3 \text{ dm}^3 \text{ mol}^{-1} \text{ s}^{-1} \qquad \textbf{(17)}^{16}$$

Consequently, the $OH^{\bullet}$ radical is converted into the $NO_3^{\bullet}$ radical, which reacts more rapidly with Np(V).[1,3,10] The initial yields from our stochastic calculations are in agreement with this quantitative radical conversion, whereas the static initial G-values used by Mincher *et al.*[1] ($G(OH^{\bullet}) = 4.12$) are almost double that found for pure water ($G(OH^{\bullet}) = 2.5$ in pure water[17]). The high G-values required to get the model agreement with this experiment are inconsistent in terms of mass-balance for this particular chemical environment.

Table 3. Comparison of calculated radiolytic yields at 10 μs for the gamma radiolysis of aerated aqueous 4.0 mol dm^{-3} HNO_3 solutions with those used by Mincher *et al.*[1]

Species	**radiolytic yields** (species 100 eV^{-1})*	
	stochastic calculation at 10 μs	Mincher *et al.*
$OH^{\bullet}$	-	4.12
$H^{\bullet}$	-	0.42
H_2	0.06	0.21
H_2O_2	0.47	0.52
$HO_2^{\bullet}$	0.02	-
O_2	0.30	-
O	1.41	-
$NO_3^{\bullet 2-}$	3.52	5.1
$NO_3^{\bullet}$	3.49	-
$NO_2^{\bullet}$	0.80	-
HNO_2	1.41	1.29

* 1 species 100 eV^{-1} = 0.096 μmol J^{-1}

Secondly, the initial yields used by Mincher *et al.* did not include any contribution from the direct effects of radiation on NO_3^- and HNO_3 (reactions **18** to **21**).[8]

$$NO_3^- \rightsquigarrow NO_3^-{}^* \rightarrow NO_2^- + O \quad (\mathbf{18})$$

$$NO_3^- \rightsquigarrow NO_3^-{}^* \rightarrow NO_3^{\bullet} + e^- \quad (\mathbf{19})$$

$$HNO_3 \rightsquigarrow HNO_3^* \rightarrow HNO_2 + O \quad (\mathbf{20})$$

$$HNO_3 \rightsquigarrow HNO_3^* \rightarrow NO_3^{\bullet} + e^- + H_{aq}^+ \quad (\mathbf{21})$$

The direct effects of radiation involve the transfer of radiation energy into the valence electrons of the solute species, in this case NO_3^- and HNO_3. The extent of direct radiation effects are usually described through the concept of electron fractions (f_s), which assumes that energy deposited in a radiation track is partitioned between the constituents of the system proportional to their respective electron fractions.[18] In 4.0 mol dm^{-3} HNO_3, the total electron fraction of NO_3^- and HNO_3 is ~19% relative to H_2O. This oversight of direct effects may explain their use of an

unrealistically high initial G($OH^{\bullet}$) value, to compensate for a lack of generated $NO_3^{\bullet}$, which is important in determining both the valency distribution of neptunium and the yield of HNO_2. The latter chemistry has recently been demonstrated by Garaix *et al.*[15] Conversely, the multi-scale modelling approach incorporates direct effect yields, derived from Jiang *et al.*[8] and correctly weighted for the respective electron fractions of NO_3^-, HNO_3, and H_2O, to provide an initial G($NO_3^{\bullet}$) value of 3.49 for 4.0 mol dm^{-3} HNO_3.

Finally, the initial yields for reduced nitrate ($NO_3^{\bullet 2-}$) and nitrous acid are crucial for determining the rate of Np(VI) reduction. The proton (H_{aq}^+) and NO_3^- anion are extremely efficient electron scavengers, such that in 4.0 mol dm^{-3} HNO_3 essentially all of the available electrons (both pre-solvated and solvated) are scavenged by these two species, ultimately being converted into reduced nitrate intermediates, reactions **22** to **25**.

$H_{aq}^+ + e_{aq}^- \rightarrow H^{\bullet}$ $\quad k = 2.3 \times 10^{10}\ dm^3\ mol^{-1}\ s^{-1}$ (**22**)[19]

$NO_3^- + e_{pre}^- \rightarrow NO_3^{\bullet 2-}$ $\quad k = 1 \times 10^{13}\ dm^3\ mol^{-1}\ s^{-1}$ (**23**)[20]

$NO_3^- + e_{aq}^- \rightarrow NO_3^{\bullet 2-}$ $\quad k = 9.7 \times 10^{9}\ dm^3\ mol^{-1}\ s^{-1}$ (**24**)[19]

$NO_3^- + H^{\bullet} \rightarrow HNO_3^-$ $\quad k = 5.6 \times 10^{6}\ dm^3\ mol^{-1}\ s^{-1}$ (**25**)[21]

The previous calculations performed by Mincher *et al.* used an initial G($NO_3^{\bullet 2-}$) value of 5.1, which equates to the total ionization of water. This value is unrealistically high, as it overcompensates for the lack of geminate and non-geminate ion-pair recombination or electron fraction weighting. This overestimation ultimately leads to too much HNO_2 being produced in the system. Interestingly, their previous experimentally derived value for G(HNO_2) is in relatively good agreement with that calculated here (8.5% difference), providing confidence in both experimental measurements and stochastic calculations.

Despite the differences in initial radiolytic yields, the multi-scale modelling approach arrives at rates coefficients for the key neptunium reactions that are similar to those previously reported for Np(VI)/Np(V) in 4.0 mol dm^{-3} HNO_3, as shown in **Table 4**.

Table 4. Optimized rate coefficients from multi-scale modelling for key neptunium reactions as a function of nitric acid concentration.

[HNO_3] (mol dm^{-3})	**ionic strength**	**rate coefficient** (dm^3 mol^{-1} s^{-1})			
		Np(VI) + HNO_2	Np(VI) + H_2O_2	Np(V) + $NO_2^{\bullet}$	Np(V) + $NO_3^{\bullet}$
0.1	0.11	1942	1.9	3.1×10^4	8.1×10^8
0.5	0.50	73	1.9	3.1×10^4	8.1×10^8
1.0	0.99	12	1.9	2.4×10^2	8.1×10^8
2.0	1.93	10	1.9	2.4×10^2	8.1×10^8
4.0	3.48	0.7	1.9	2.4×10^2	8.1×10^8
6.0	4.50	0.7	1.9	2.4×10^2	8.1×10^8

However, the multi-scale modelling approach provides significantly more mechanistic confidence in the intricate chemical processes occurring from the point of energy deposition to steady-state species concentrations. The neptunium valency distribution attained in gamma irradiated 4.0 mol dm^{-3} HNO_3 begins with an initial increase in the concentration of Np(VI), predominantly due to the oxidation of Np(V) by $NO_3^{\bullet}$. This is followed by progressive reduction of Np(VI) to Np(V) by HNO_2 and H_2O_2, the prior of which has the largest contribution. The delay in net Np(VI) reduction is due to the need for both HNO_2 and H_2O_2 to accumulate to sufficiently high concentration. Ultimately a Np(VI):Np(V) ratio of 1.6 is attained at ~18.5 kGy.

Neptunium Valency Distribution Dependency on Nitric Acid Concentration. The valency distribution of neptunium in 6.0 (**A**), 2.0 (**B**), 1.0 (**C**), and 0.5 (**D**) mol dm^{-3} HNO_3 solutions is shown in **Figure 3**. As the concentration of nitric acid decreases the dynamics of the neptunium valency distribution significantly alters: (i) the initial increase in Np(VI) concentration becomes less pronounced and shorter lived, until eventually ceasing entirely; and (ii) reduction of Np(VI) becomes faster and more extensive, leading to an inversion in the initial oxidation state populations at lower doses. For example, in 1.0 mol dm^{-3} HNO_3 the neptunium valency populations invert at ~12 kGy, resulting in a Np(VI):Np(V) ratio of 0.6 at ~27 kGy, whereas in 0.5 mol dm^{-3} HNO_3, population inversion occurs at ~6.6 kGy, resulting in a Np(VI):Np(V) ratio of 0.26 at ~35 kGy. As the concentration of nitric acid is lowered, contributions from direct radiation effects become progressively smaller (lower NO_3^-/HNO_3 electron fractions) and the

concentration of undissociated HNO_3 decreases, both of which leads to smaller initial radiolytic yields of $NO_3^{\bullet}$, e.g. $G(NO_3^{\bullet}) = 1.16$ and 0.67 for 1.0 and 0.5 mol dm^{-3} HNO_3, respectively. Although a reduction in $G(NO_3^{\bullet})$ is complemented by a proportional increase in $G(OH^{\bullet})$, the $OH^{\bullet}$ radical reacts more slowly with Np(V) than $NO_3^{\bullet}$, which manifests as the progressive loss in the initial growth in Np(VI) concentration.[10] Ultimately this leads to a greater preference of Np(V) over Np(VI).

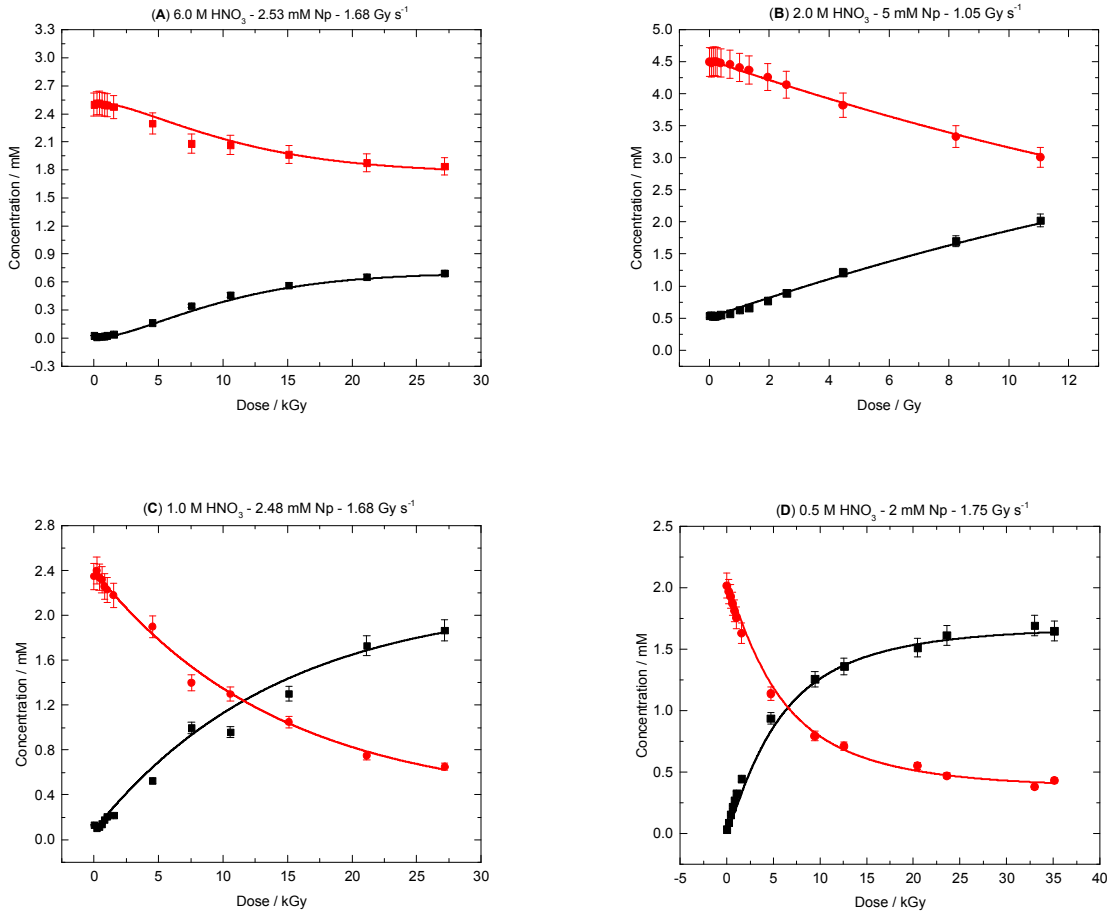

Figure 2. Concentration of Np(V)(■) and Np(VI)(●) (±5% error bars) as a function of absorbed dose from the gamma radiolysis of: (**A**) 6.0 mol dm^{-3} HNO_3 + 2.53 × 10^{-3} mol dm^{-3} Np; (**B**) 2.0 mol dm^{-3} HNO_3 + 4 × 10^{-3} mol dm^{-3} Np; (**C**) 1.0 mol dm^{-3} HNO_3 + 2.48 × 10^{-3} mol dm^{-3} Np; (**D**) 0.5 mol dm^{-3} HNO_3 + 2.05 × 10^{-3} mol dm^{-3} Np. Solid lines are predicted values from multi-scale modelling calculations described in this work. Np(V) concentrations corrected for mass balance.

Neptunium in 0.1 mol dm^{-3} Nitric Acid. The valency distribution of neptunium in 0.1 mol dm^{-3} HNO_3 solutions is shown in **Figure 3**. The rate of Np(VI) reduction is significantly faster than all

other nitric acid concentrations, and cannot be mechanistically explained based on the previously presented radical and molecular mechanisms. We should, in theory, see a relatively higher rate of Np(VI) reduction due to the reduced formation of $NO_3^{\bullet}$ by both direct and indirect radiation pathways. However, the increasing rate of Np(VI) reduction with decreasing nitric acid concentration is not linear, as a reduction in $G(NO_3^{\bullet})$ is compensated for by an increase in $G(OH^{\bullet})$.

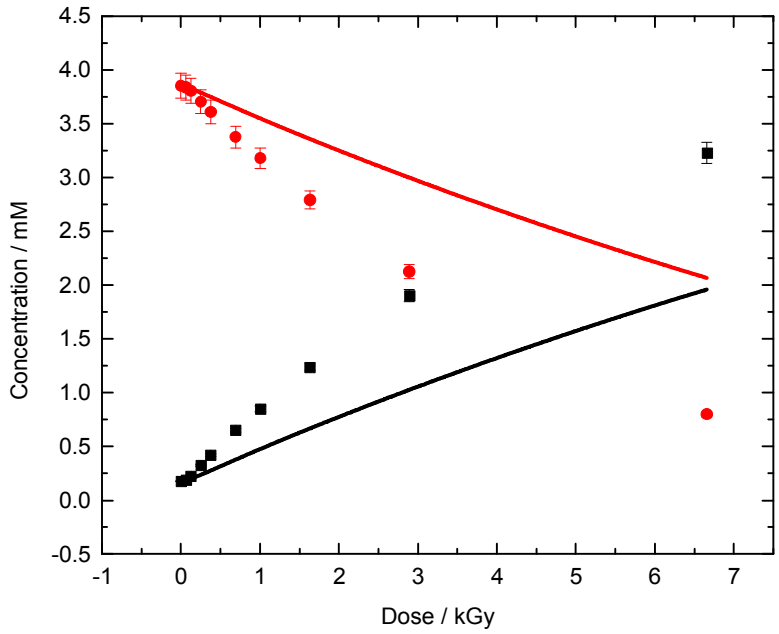

Figure 3. Concentration of Np(V)(■) and Np(VI)(●) (±5% error bars) as a function of absorbed dose from the gamma radiolysis (1.05 Gy s^{-1}) of 0.1 mol dm^{-3} HNO_3 + 4 × 10^{-3} mol dm^{-3} Np. Solid lines are predicted values from multi-scale modelling calculations described in this work.

The concentration conversion of Np(VI) to Np(V) within the investigated dose range cannot be explained by the available concentrations of reducing radiolytic species. The corresponding calculated initial yields are given in **Table 5**, comparing the total initial concentration prior to bulk chemistry at 2.89 kGy. For this 0.1 mol dm^{-3} HNO_3 system, at 2.89 kGy 1.72 × 10^{-3} mol dm^{-3} of Np(VI) has been reduced (43%), but the total amount of radiolytic species formed within the radiation track only equals 2.59 × 10^{-3} mol dm^{-3}, of which by definition only half are reducing species (1.30 × 10^{-3} mol dm^{-3}). Therefore, even if all of the reducing species and none of the oxidizing species reacted with Np(VI), and we ignore all other

bulk chemistry processes, we would still be unable to account for the measured amount of reduced Np(VI) by 24%.

Table 5. Calculated initial radiolytic yields at 10 μs and maximum initial concentrations of the primary radiation track products at 2.89 kGy for the gamma radiolysis of aerated aqueous 0.1 mol dm^{-3} HNO_3 solutions.

Species	**radiolytic yields** (species 100 eV^{-1})*	**maximum initial concentration** (mol dm^{-3})
$OH^{\bullet}$	3.12	9.35×10^{-4}
H_2	0.32	9.59×10^{-5}
H_2O_2	0.81	2.43×10^{-4}
$HO_2^{\bullet}$	0.31	9.29×10^{-5}
O_2	0.03	8.99×10^{-6}
O	0.04	1.20×10^{-5}
$NO_3^{\bullet 2-}$	1.88	5.63×10^{-4}
$NO_3^{\bullet}$	0.05	1.50×10^{-5}
$NO_2^{\bullet}$	2.08	6.23×10^{-4}
HNO_2	0.02	5.99×10^{-6}

* 1 species 100 eV^{-1} = 0.096 μmol J^{-1}

Further attempts to model this system provided additional insight. Firstly, the optimized rate coefficient (k = 1942 dm^3 mol^{-1} s^{-1}) given in **Table 4** for the reduction of Np(VI) by HNO_2 is unrealistically high, but this value is a consequence of the strained conditions required to attain the maximum reducing capability under these conditions (i.e. both track and bulk homogeneous chemistry). This high rate coefficient is still insufficient to achieve agreement with experiment and further increases did not give and further change. Secondly, the process responsible for the rapid reduction in Np(VI) at 0.1 mol dm^{-3} HNO_3 must be inhibited by acidity, as Np(VI) reduction to this extent was not observed for nitric acid concentrations ≥0.5 mol dm^{-3}. It was found that excellent agreement between calculation and experiment could be attained by completely removing $OH^{\bullet}$ and $NO_3^{\bullet}$ radicals from the system by using a side-mechanism with a potential contaminant at a pseudo-first order rate of ~1×10^5 s^{-1}. However, this potential contaminant would have to: (i) be unreactive towards Np(V) and Np(VI), as there is no change in

their respective concentrations in the associated control experiments; and (ii) possess a concentration >1 × 10^{-3} mol dm^{-3} in order to compete with Np(V) for $OH^{\bullet}$ and $NO_3^{\bullet}$. This level of contamination is highly unlikely considering the neptunium sample preparation procedure used in this work. Finally, there could be a pH dependent Np(VI) catalytic reduction process occurring. However, the identity of the pathway is unknown and further work is necessary to determine the feasibility of this additional pH dependent catalytic mechanism.

Evaluation of Optimized Rate Coefficients. The optimized rate coefficients in **Table 4** show that the neptunium valency distribution is most sensitive to the reduction of Np(VI) by HNO_2 throughout the whole nitric acid concentration range, and to a lesser extent the oxidation of Np(V) by $NO_2^{\bullet}$. Both of these rate coefficients are essential for establishing high dose/long timescale steady-state oxidation state distributions. However, the rate coefficients for both reactions decrease as a function of nitric acid concentration, by up to two orders of magnitude. A similar trend was reported by Vladimirova despite her finding considerably different magnitudes.[3] Although ionic strength impacts could be proposed for some of these changes, our modelling efforts suggest that the decrease in rate coefficients most likely reflects the overcompensation necessary to account for the postulated catalytic Np(VI) reduction process. As the concentration of nitric acid increases the rate coefficients for these two reactions converge, implying that the process occurring at 0.1 mol dm^{-3} has an influence up to ~4 mol dm^{-3}. In contrast, the rate coefficients for H_2O_2 and $NO_3^{\bullet}$ were found to be constant throughout the investigated nitric acid concentration range, with the rate of the latter value being consistent with Mincher *et al.*[1] For the 6.0 mol dm^{-3} HNO_3 Np(VI)/Np(V) irradiation, given in **Figure 2** (**A**), an additional reaction for the oxidation of Np(V) by HNO_3 was necessary to be included in the reaction set. The thermal oxidation of Np(V) by HNO_3 has been the subject of multiple investigations over many decades, leading to a variety of mechanistic interpretations and derived kinetics, the majority of which are highly complex and inconsistent with one another.[22-26] The mechanism employed in the presented calculations utilizes the non-elementary process (Np(V) + HNO_3 → Np(VI) + HNO_3^-) with an optimized rate coefficient of 2.0 × 10^{-3} dm^3 mol^{-1} s^{-1}.

CONCLUSIONS

The gamma-induced radiation chemistry of neptunium-nitric acid solutions has been re-evaluated over a range of doses (0 – 40 kGy) and nitric acid (0.1 – 6.0 mol dm^{-3}) concentrations using a multi-scale modelling approach. The observed Np(VI):Np(V) oxidation-state distribution was found to depend on the reactions of neptunium with both the reducing and oxidizing products from aqueous nitric acid radiolysis, especially HNO_2, H_2O_2, $NO_2^{\bullet}$, and $NO_3^{\bullet}$.

Over the nitric acid concentration range 0.5 to 6.0 mol dm^{-3} the concentration of Np(VI) initially increases, and the dose at which net reduction occurs is progressively delayed. This is due to the formation of increasing amounts of $NO_3^{\bullet}$ by both direct and indirect radiation effects, where oxidation of Np(V) by $NO_3^{\bullet}$ ($k = 8.1 \times 10^8$ dm^3 mol^{-1} s^{-1}) provides the initial increase in Np(VI) concentration. Consumption of HNO_2 by $NO_3^{\bullet}$ reduces the concentration of HNO_2 available for reduction of Np(VI). The reduction of Np(VI) is dominated by thermal reactions with HNO_2 ($k = 0.7 – 73$ dm^3 mol^{-1} s^{-1}) and H_2O_2 ($k = 1.9$ dm^3 mol^{-1} s^{-1}). The steady-state Np(VI):Np(V) oxidation-state distribution is finally established once the concentration of Np(V) is sufficiently high enough to be oxidized by $NO_2^{\bullet}$ ($k = 2.4 \times 10^2 – 3.1 \times 10^4$ dm^3 mol^{-1} s^{-1}). The 6.0 mol dm^{-3} HNO_3 condition requires an additional thermal oxidation reaction of Np(V) by 'HNO_3' ($k = 2.0 \times 10^{-3}$ dm^3 mol^{-1} s^{-1}).

However, the multi-scale modelling of 0.5 to 6.0 mol dm^{-3} HNO_3 systems is not sufficient to explain the experimental radiation chemical behavior of neptunium in 0.1 mol dm^{-3} HNO_3. At this acid concentration the rate of Np(VI) reduction is in excess of that which can be accounted for by radiolytic product mass balance, suggesting the existence of a catalytic acid dependent reduction process. This additional catalytic process is attributed for the cause of the range exhibited by the optimized rate coefficients for HNO_2 and $NO_2^{\bullet}$.

AUTHOR INFORMATION

Corresponding Author:

E-mail: gregory.p.horne@gmail.com.

Mobile Number: (+1) 5742526022

ACKNOWLEDGEMENTS

This research has been funded by the US-DOE Assistant Secretary for NE, under the FCR&D Radiation Chemistry program; DOE-Idaho Operations Office Contract DE-AC07-05ID14517 and DE-NE0008406 grant.

REFERENCE

(1) Mincher, B.; Precek, M.; Mezyk, S. P.; Elias, G.; Martin, L. R.; Paulenova, A. The Redox Chemistry of Neptunium in γ-Irradiated Aqueous Nitric Acid. *Radiochim. Acta.*, **2013**, 101, 259-265.

(2) Tochiyama, O.; Nakamura, Y.; Katayma, Y.; Inoue, Y. Equilibrium of Nitrous Acid-Catalyzed Oxidation of Neptunium in Nitric Acid-TBP Extraction System. *J. Nucl. Sci. Tech.*, **1995**, 32, 50-59.

(3) Vladimirova, M. V. Recent Achievements of Actinide Radiation Chemistry. *J. Alloys Comp.*, **1998**, 271-273, 723-727.

(4) Horne, G. P.; Donoclift, T. A.; Sims, H. E.; Orr, R. M.; Pimblott, S. M. Multi-Scale Modelling of the Gamma Radiolysis of Nitrate Solutions. *J. Phys. Chem. B*, **2016**, *submitted*.

(5) Pimblott, S. M.; LaVerne, J. A.; Mozumder, A. Monte Carlo Simulation of Range and Energy Deposition by Electrons in Gaseous and Liquid Water. *J. Phys. Chem.*, **1996**, *100*, 8595-8606.

(6) Pimblott, S.M.; LaVerne, J. A. Effects of Track Structure on the Ion Radiolysis of the Fricke Dosimeter. *J. Phys. Chem. A*, **2002**, *106*, 9420-9427.

(7) Clifford, P.; Green, N. J. B.; Oldfield, M. J.; Pilling, M. J. ; Pimblott, S. M. Stochastic Models of Multi-Species Kinetics in Radiation-Induced Spurs. *J. Chem. Soc., Faraday Trans.*, **1986**, *82*, 2673-2689.

(8) Jiang, P.Y.; Nagaishi, R.; Yotsuyanagi, T.; Katsumura, Y.; Ishigure, K. Gamma Radiolysis Study of Concentrated Nitric Acid Solutions. *J. Chem. Soc. Faraday Trans.*, **1994**, 90, 93-95.

(9) Tachimori, S. Numerical Simulation for Chemical Reactions of Actinide Elements in Aqueous Nitric Acid Solution. *J. Nucl. Sci. Tech.*, **1991**, 28, 218-227.

(10) Gogolev, A. V.; Shilov, V. P.; Fedoseev, A. M. I. E.; Pikaev, A. K. A Pulse Radiolysis Study of the Reactivity of Neptunyl Ions Relative to Inorganic Free Radicals. *Russ. Chem. Bull.*, **1986**, 35, 422-424.

(11) Pikaev, A. K.; Shilov, V. P.; Gogolev, A. V. Radiation Chemistry of Aqueous Solutions of Actinides. *Russ. Chem. Rev.*, **1997**, 66, 763-788.

(12) Vladimirova, M. V. Mathematical Modelling of the Radiation-Chemical Behavior of Np in Nitric Acid. Equilibrium States. *Radiokhimiya*, **1995**, 37, 446-452.

(13) Fricke, H.; Hart, E. J. The Oxidation of Fe^{2+} to Fe^{3+} by the Irradiation with X-Rays of Solutions of Ferrous Sulfate in Sulfuric Acid. *J. Chem. Phys.*, **1935**, 3, 60-61.

(14) Davis, W.; De Bruin, H. J. New Activity Coefficients of 0 – 100 Per Cent Aqueous Nitric Acid. *J. Inorg. Nucl. Chem.*, **1964**, 26, 1069-1083.

(15) Garaix, G.; Horne, G. P.; Venault, L.; Moisy, P.; Pimblott, S. M.; Marignier, J. -L.; Mostafavi, M. Decay Mechanism of $NO_3^{\bullet}$ Radical in Highly Concentrated Nitrate and Nitric Acidic Solutions in the Absence and Presence of Hydrazine. *J. Phys. Chem. B*, **2016**, 120, 5008−5014.

(16) Poskrebyshev, G. A.; Neta, P.; Huie, R. E. Equilibrium Constant of the Reaction $OH^{\bullet}$ + $HNO_3 \leftrightarrows H_2O + NO_3^{\bullet}$ in Aqueous Solution. *J. Geophys. Res.*, **2001**, 106, 4995−5004.

(17) Elliot, A. J.; Bartels, D. M. The Reaction Set, Rate Constants and G-Values for the Simulation of the Radiolysis of Light Water Over the Range 20° to 350°C Based on Information Available in 2008. *AECL Nuclear Platform Research and Development – Report 153-127160-450-001*. **2009**.

(18) Swallow, A. J.; Inokuti, M. Radiation-Energy Partition Among Mixture Components: Current Ideas on an Old Question. *Radiat. Phys. Chem.*, **1988**, 32, 185−189.

(19) Buxton, G. V.; Greenstock, C. L.; Helman, W. P. Ross, A. B. Critical Review of Rate Constants for Reactions of Hydrated Electrons, Hydrogen Atoms and Hydroxyl Radicals ($^{\bullet}OH/^{\bullet}O^{-}$) in Aqueous Solution. *J. Phys. Chem. Ref. Data*, **1988**, 17, 513-886.

(20) Pimblott, S. M.; LaVerne, J. A. On the Radiation Chemical Kinetics of the Precursor to the Hydrated Electron. *J. Phys. Chem. A*, **1998**, 102, 2967-2975.

(21) Mezyk, S. P.; Bartels, D. M. Direct EPR Measurement of Arrehenius Parameters for the Reactions of $H^{\bullet}$ Atoms with H_2O_2 and $D^{\bullet}$ Atoms in Aqueous Solution. *J. Chem. Soc. Faraday Trans.*, **1995**, 91, 3127-3132.

(22) Zhang, H.; Liu, Z-H.; Li, L.; Yang, H.; Ye, G-A.; Zhou, X-M.; Wang, R. The Reversible Reaction Kinetics of Neptunium with Nitrous and Nitric Acids. *J. Radioanal. Nucl. Chem.*, **2016**, 308, 123-128.

(23) Siddall, T. H.; Dukes, E. K. Kinetics of HNO_2 Catalyzed Oxidation Reaction of Neptunium(V) by Aqueous Solution of Nitric Acid. *J. Am. Chem. Soc.*, **1959**, 81, 790-794.

(24) Tochiyama, O.; Nakamura, Y.; Katayama, Y.; Inque, Y. Equilibrium of Nitrous Acid-Catalysed Oxidation of Neputunium in Nitric Acid TBP Extraction System. *J. Nucl. Sci. Tech.*, **1995**, 32, 50-59.

(25) Tochiyama, O.; Nakamura, Y.; Hirota, M.; Inoue, Y. Kinetics of Nitrous Acid-Catalysed Oxidation of Neptunium in Nitric Acid TBP Extraction System. *J. Nucl. Sci Tech.*, **1995**, 32, 118-124.

(26) Marchenko, V. I.; Koltunov, V. S.; Dvoeglazov, K. N. Kinetics and Mechanisms of Redox Reactions of U, Pu, and Np in Tributyl Phosphate Solutions. *Radiochemistry*, **2010**, 52, 111-126.